Ground and Excited States of Hemoglobin CO and Horseradish Peroxidase CO: SAC/SAC-CI Study

Y. Tokita[†,§] and H. Nakatsuji*[,†,‡]

Department of Synthetic Chemistry and Biological Chemistry, Faculty of Engineering, Kyoto University, Sakyo-ku, Kyoto, 606-01 Japan, The Institute for Fundamental Chemistry, 34-4 Takano Nishi-Hikari-cho, Sakyo-ku, Kyoto, 606 Japan, and Research Center, Denki Kagaku Kogyo Co., Ltd., 3-5-1 Asahimachi, Machida-shi Tokyo, 194 Japan

Received: November 14, 1996; In Final Form: February 5, 1997[⊗]

The SAC (symmetry adapted cluster)/SAC-CI method is applied to the calculations of the ground and excited states of carboxyheme complexes with two kinds of proximal ligands, imidazole (model hemoglobin and myoglobin) and imidazolate (model peroxidases). The Mulliken population analysis for the ground state of horseradish peroxidase CO (HRPCO) shows that the electron push effect from proximal to distal sites causes a charge polarization between the distal ligand and CO in comparison with the model hemoglobin CO (HbCO). The excited states of the HbCO and HRPCO are calculated up to 7.8 and 7.1 eV, respectively. The calculated excitation energies and oscillator strengths correspond well with the observed electronic spectra of these two compounds. The Q bands are well described by the excitations within Gouterman's four orbitals. The higher side shoulder of the B band is named as the n band since it is assigned to a distinct electronic structure. For the B, n, N, L, and M bands, Gouterman's four orbitals plus some lower porphyrin π orbitals give dominant contributions. The states higher than the M band are characterized by the d−π*, π−d*, d−CO*, and π−CO*, etc., and therefore their intensities are predicted to be small. Some important differences in the excited states of HRPCO and HbCO are observed. In HRPCO, the lower porphyrin π orbitals mix with imidazole σ orbitals and are unstabilized, so that the B band energy is lower than that of HbCO, and the nature of the N band is very different between them. The different peaks in the spectrum of HbCO are correlated with those of free-base porphine (FBP) and Mg−porphine (MgP) studied previously in our laboratory.

I. Introduction

Hemoglobin and myoglobin play important roles in mammalian life particularly in oxygen transport and storage. Hemoglobin is found packed in high concentrations in red blood cells and myoglobin in aerobic muscle tissue. On the other hand, peroxidases, HRP (horseradish peroxidase) and CCP (cytochrome *c* peroxidase), etc., are widely distributed in the biological systems. They are discovered in many plants, in some animal tissues, and in microorganisms.[1] The peroxidase reaction accompanies two electron oxidation−reduction, but it normally proceeds in four distinct steps:

$$\mathrm{E} + \mathrm{ROOH} \rightarrow \text{compound I} + \mathrm{ROH}$$

$$\text{compound I} + \mathrm{AH_2} \rightarrow \text{compound II} + \mathrm{AH^\bullet}$$

$$\text{compound II} + \mathrm{AH_2} \rightarrow \mathrm{E} + \mathrm{AH^\bullet}$$

$$\mathrm{AH^\bullet} + \mathrm{AH^\bullet} \rightarrow \text{nonradical products}$$

where E represents the native peroxidase. Compound I is two oxidation equivalents above the native enzyme and believed to be a Fe(IV) low-spin ($S = 1$) oxoporphyrin π cation radical ($S = 1/2$) complex[2] introduced by heterolytic O−O bond cleavage, and compound II is one oxidation equivalent above the native enzyme and is a Fe(IV) low-spin ($S = 1$) oxoporphyrin species.[3] Furthermore, compound I is also believed to be formed in the reactions of the various function oxygenase, the cytochrome P450s.[4] The oxidations catalyzed by the putative Fe−oxo species in P450 are different from those of the peroxidases. In P450s, compound I species transfer a single atom of oxygen directly to a variety of substrates.

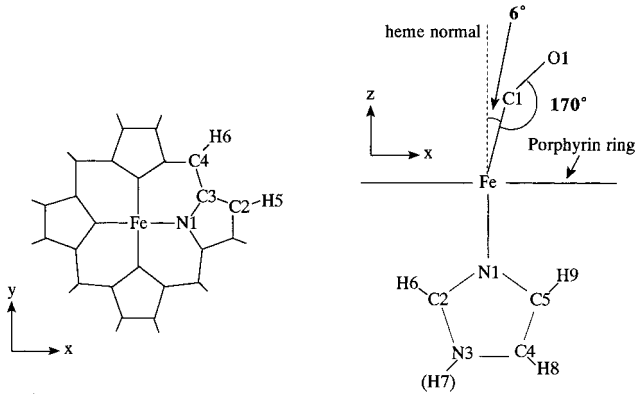

Figure 1. Geometry of HbCO and HRPCO. The numbering of atoms corresponds to those shown in Table 1.

One of the reasons for having these different functions is believed to lie in the difference in the proximal ligand. In hemoglobin and myoglobin, the proximal ligand is a neutral imidazole as a histidine residue. In peroxidases, on the other hand, the proximal ligand is an anionic imidazolate, because the H7 proton of the proximal imidazole (Figure 1) is hydrogen-bonded by the amino acid residue (Asp235 in CCP) and can easily be dissociated in the protein environment.[5] In addition, in P450s, the proximal ligand is a thiolate as a cysteine residue.[6] Thus, the oxidation activity seems to be dependent upon whether the active center, heme, has an anionic proximal ligand or not. Here we focus on the heme−CO complexes and study the

* To whom correspondence should be addressed.
† Kyoto University.
‡ The Institute for Fundamental Chemistry.
§ Denki Kagaku Kogyo Co., Ltd.
⊗ Abstract published in *Advance ACS Abstracts,* April 1, 1997.

S1089-5647(96)03805-9 CCC: $14.00 © 1997 American Chemical Society

TABLE 1: Atomic Coordinates of HbCO and HRPCO (Å)

segment	atom[a]	*x*	*y*	*z*	segment	atom[a]	*x*	*y*	*z*
porphine	N1	1.9537	0.0	0.0	imidazole	N1	0.0	0.0	−2.0654
	C2	4.1889	0.6915	0.0		C2	−1.2095	0.0	−2.7916
	C3	2.8060	1.1297	0.0		N3	−0.8706	0.0	−4.2036
	C4	2.4702	2.4702	0.0		C4	0.5376	0.0	−4.2391
	H5	5.0604	1.3294	0.0		C5	1.0562	0.0	−2.9478
	H6	3.2339	3.2339	0.0		H6	−2.2826	0.0	−2.6693
CO[b]	C1	0.1850	0.0	1.7603		H7[c]	−1.5281	0.0	−5.0604
	O1	0.5020	0.0	2.8658		H8	1.0035	0.0	−5.2134
iron	Fe	0.0	0.0	0.0		H9	2.0637	0.0	−2.5587

[a] The numberings of atoms in each segment are given in Figure 1. [b] The lengthes of Fe−C1, C1−O1, Fe−N(por), and Fe−N(Im) are 1.77, 1.15, 1.95, and 2.07 Å, respectively. The Fe−C1−O1 angle and the angle between Fe−C and heme normal are 170° and 6°, respectively. [c] The H7 atom on imidazole is removed in HRPCO.

proximal ligand effect. It is known that the B band energy decreases with increasing the negativity of the proximal ligand.

The physiological function of HbCO in the presence of significant concentrations of CO has been the focus of considerable research interest.[7] Although the bonding of an O_2 molecule to free porphyrin is further stabilized by a hydrogen bond between the terminal oxygen atom and the neighboring proteins,[8] a poisoning molecule, CO, binds to free porphyrin much more strongly than the O_2 molecule and gives HbCO.

Recent experimental reports on HbCO clarified the crystal structure,[9] and the nature of the Fe−C−O bonding using resonance Raman spectroscopy.[10] Theoretical studies on HbCO have been carried out by semiempirical,[11,12] ab initio,[13,14] and Xα[11] methods. However, knowledge of the electronic structures of the ground and excited states of HbCO is still incomplete. Recently, we have reported a preliminary result on the ground and excited states of HbCO[15,16a] using the SAC (symmetry adapted cluster)[17] theory for the ground state and the SAC-CI theory for the excited states.[18] It was found that elaborate studies including a large amount of electron correlations are necessary for a sound and reliable understanding of the electronic structures of the ground and excited states of HbCO. This is also true from our recent studies on the ground and excited states of porphyrins: free-base porphine,[19] Mg porphine,[20] tetraazaporphine,[21a] phthalocyanine,[21b] and oxyheme.[22] We report here our studies on the ground and excited states of HbCO and HRPCO using the SAC/SAC-CI method. The focus is on the effect of the proximal ligand, which is different between HbCO and HRPCO. The accuracy and the effectiveness of the SAC/SAC-CI method is now well established,[16] and the SAC/SAC-CI code[23] is available on request.

II. Methods

The carboxyheme models, HbCO ($FeC_{24}N_6OH_{16}$; carbonyl iron(II)porphyrin(imidazole)) and HRPCO ($FeC_{24}N_6OH_{15}$; carbonyl iron(II)porphyrin(imidazolate)), consist of 236 electrons and 48 and 47 atoms, respectively, and the geometries are shown in Table 1 and Figure 1. We adopted X-ray crystallographic data for human carbon monoxyhemoglobin[9a] with a small modification; the porphyrin skeleton is modified to have D_{4h} symmetry, and the imidazole plane, one of the $N_{por}-Fe-N_{por}$ axes, and the C−O axis are put on a mirror plane, as shown in Figure 1. The entire molecular symmetry is C_s and the porphyrin is put on the *xy* plane. Other geometrical parameters are taken from those used previously for oxyheme.[22] Note that the Fe−C1 bond is not on the normal line of the porphyrin ring; the angle from the normal line is 6°. Further, the CO bond is not on the line of the Fe−C1 bond: the Fe-C1-O1 angle is 170°. Such a bending structure of CO was supported by ab initio calculations.[13] In HRPCO, the geometry is the same as in HbCO except that the H7 proton (Figure 1) is removed from the proximal imidazole ligand.

TABLE 2: Dimensions of the Linked Terms for the SAC/SAC-CI Calculations of the Singlet States of HbCO and HRPCO

model	state	before selection	N^a	after selection
HbCO	SAC			
	A′	347 066 19	1	16 664
	SAC-CI			
	A′	347 066 19	5	92 350
	A″	346 716 90	5	120 182
HRPCO	SAC			
	A′	342468 56	1	16 335
	SAC-CI			
	A′	342 468 56	5	86 855
	A″	342 156 94	5	93 006

[a] *N* denotes the number of reference configurations used in the configuration selection scheme.

The quality of the GTO basis functions used here is the same as that used previously for the calculations of porphyrins.[15,19−22] For the Fe atom, we use the Huzinaga's (5333/53/5)/[53321/53/41] set[24] plus p-type polarization functions (α = 0.082), for C, N, and O, the (63/5)/[63/41] set[24] plus a p-type anion basis (α = 0.059) for oxygen, and for H the (4)/[4] set.[25] The basis set for imidazole is minimal: for C and N, the (63/5)/[63/5] set[24] and for H the (4)/[4] set.[25] The total numbers of contracted GTOs are 278 in HbCO and 277 in HRPCO. Since most excitations studied in this paper are within the porphyrin ring, the effect of the mixed-quality basis set should be small, although it may not be negligible for the excitations involving the ligands.

The SAC/SAC-CI calculations were carried out using SAC85[23a] and its modified version.[23b] The HF molecular orbitals (MOs) were used as reference orbitals. A total of 229 MOs in HbCO and 228 MOs in HRPCO were used as active MOs: all valence orbitals were included in the active space, and only the 1s orbitals of C, N, and O atoms and the core orbitals (1s, 2s, 2p, 3s, and 3p) of Fe were treated as frozen cores. All the single excitations and the selected double excitations within this active space constitute the linked operators, and their products the unlinked operators. The perturbative configuration selection procedure[19,26] was performed with the energy threshold 1×10^{-5} au for the excitations within the π space and 2×10^{-5} au for others for the ground state, and for the excited states with the threshold 5×10^{-7} au for the excitations within the π space and 1×10^{-6} au for others. The resultant dimensions for the SAC/SAC-CI calculations are shown in Table 2.

III. Electronic Structure of the Ground State

First we analyze the HF orbitals for the ground state. The HF orbital energy and character are shown in Table 3 for HbCO and Table 4 for HRPCO. The numbering of MOs excludes core orbitals and starts from the lowest MO in the active space. CO(π_b) and CO(π_a) denote the π-type bonding and antibonding

TABLE 3: Orbital Energies and Characters of Some HF Orbitals of HbCO

MO no.[a]	sym-metry	orbital energy (eV)	nature[b]
		Occupied Orbitals	
61	39a′	−13.378	Fe s + Fe d_{z^2} + CO(σ) + Im(σ)
62	23a″	−12.849	CO(O1[c])p_y − Fe d_{yz} + Im(π^p)
63	40a′	−12.464	CO(O1[c])p_x − Fe d_{xz} + Por(σ)
64	24a″	−12.362	CO(O1[c])p_y − Fe d_{yz} + Im(π^p) + Por(σ)
	'		
	'		
	'		
68	26a″	−12.076	Fe d_{xy}
69	27a″	−11.671	Fe d_{yz} − Im(π^p)
	'		
	'		
	'		
71	43a′	−10.170	Por(π)
72	29a″	−10.011	Fe d_{yz} − Im(π^p)
73	44a′	−9.412	Por(π)
74	45a′	−9.160	Por(π)
75	46a′	−8.963	Por(π) − Fe d_{xz}
76	30a″	−8.841	Por(π) − Fe d_{yz}
77	47a′	−6.578	Por(π) (n−HOMO; 4 orbitals)
78	31a″	−6.115	Por(π) (HOMO; 4 orbitals)
		Unoccupied Orbitals	
79	32a″	+0.298	Por(π) - Fe d_{yz} (LUMO; 4 orbitals)
80	48a′	+0.327	Por(π) - Fe d_{xz} (n-LUMO; 4 orbitals)
81	33a″	+3.096	Por(π)
	'		
	'		
	'		
83	49a′	+3.893	CO(πa^o) − CO(σ) − Fe d_{z^2} − Fe $d_{x^2} - y^2$ − Por(σ)
84	35a″	+4.490	CO(πa^p) − Fe d_{yz}
85	50a′	+4.491	CO(πa^o) − Fe d_{xz} − Por(σ)
	'		
	'		
	'		
87	52a′	+5.295	CO(πa^o) − Fe $d_{x^2-y^2}$)
88	36a″	+5.341	CO(πa^p) − Fe p_y − Por(σ)
	'		
	'		
	'		
90	53a′	+5.701	CO(σ) − Fe d_{z^2} − Fe $d_{x^2-y^2}$ + Por(σ)
91	38a″	+6.019	CO(πa^p) − Por(π) − Im(π^p)
	'		
	'		
	'		
101	58a′	+9.440	CO(σ) + Fe d_{z^2} − Fe $d_{x^2-y^2}$ − Por(σ)

[a] The numbering of the HF molecular orbitals. The numbering starts from the lowest energy orbital into active space. [b] The plus (+) and minus (−) signs denote the bonding and antibonding interactions, respectively. The "πb" and "πa" denote the π-type bonding and antibonding orbitals localized at CO. The superscripts "o" and "p" denote that the orbitals are on and perpendicular to the mirror plane, respectively. [c] O1 and N3 atoms are illustrated in Figure 1.

orbitals localized at carbon monoxide. The superscripts "o" and "p" as in CO(π_b^o) and CO(π_a^p) denote that the orbitals are on and perpendicular to the mirror plane, respectively. The porphyrin π-type orbitals gather in the HOMO−LUMO region. In HbCO, the HOMO (31a″: 78), next-HOMO (47a′: 77), the LUMO (32a″: 79), and next-LUMO (48a′: 80), called the "four orbitals", are separated in energy from the other orbitals, implying the validity of the Gouterman's four-orbital model:[27] this was also observed in free-base porphine,[19] Mg−porphine,[20] and oxyheme,[22] but was not for free-base tetraazaporphine and phthalocyanine.[21] These four orbitals are mostly the porphine π orbitals, although the Fe dπ orbitals mix with the unoccupied MOs. The mixing of the CO and imidazole orbitals with the four orbitals is very small. On the other hand, in HRPCO, the orbital energies are raised up and the energy separation between

TABLE 4: Orbital Energies and Characters of Some HF Orbitals of HRPCO

MO no.[a]	sym-metry	orbital energy (eV)	nature[a]
		Occupied Orbitals	
60	38a′	−9.677	CO(O1[a])p_x − Fe d_{xz} + Fe p_x − Por(σ)
61	23a″	−9.640	CO(O1[a])p_y − Fe d_{yz} + Fe p_y + Por(σ)
62	39a′	−9.527	Fe $d_{x^2-y^2}$ + d_{xz} + Por(σ)
63	24a″	−9.479	Por(π)
64	40a′	−9.279	CO(O1[a])p_x − Fe d_{xz} + Por(σ) − Im(π^o)
65	25a″	−9.279	Fe d_{xy} + Fe d_{xz} + Por(σ) − Im(π^p)
66	26a″	−9.154	Fe d_{xy}
67	41a′	-8.354	Fe s + Fe p_z + Im(σ)
68	27a″	−7.582	Por(π)
69	42a′	−7.564	Por(π)
70	43a′	−6.830	Por(π), Im(σ)
71	44a′	−6.514	Por(π)
72	45a′	−6.259	Fe s + Fe d_{xz} + Im(σ) − Por(π)
73	28a″	−6.142	Fe d_{yz} − Por(π)
74	46a′	−6.136	Fe s + Fe d_{xz} + Im(σ) − Por(π)
75	29a″	−4.820	Fe p_y + Im(π^p) − Por(σ)
76	30a″	−4.023	Im(π^p)
77	47a′	−3.839	CO(s) − Por(π) − Im(σ) (n−HOMO)
78	31a''	−3.469	Por(π) (HOMO)
		Unoccupied Orbitals	
79	32a″	2.947	Fe d_{yz} − Por(π) (LUMO)
80	48a′	2.952	Fe d_{xz} − Por(π) (n−LUMO)
81	33a″	5.600	Por(π)
82	49a′	6.271	CO(σ) − Fe d_{z^2} + Fe $d_{x^2-y^2}$ + Por(σ)
	'		
	'		
	'		
84	34a″	6.964	CO(πa^p) + CO(σ) − Fe d_{yz} + Fe p_y − Por(σ)
85	51a′	7.358	CO(πa^o) + Fe $d_{x^2-y^2}$ − Fe dz2 − Fe p_x
86	35a″	7.410	CO(πa^p) + Fe p_y
	'		
	'		
	'		
88	53a′	8.197	CO(πa^o) + CO(O1[a]) p_z − Fe $d_{x^2-y^2}$ − Fe d_{z^2} + Por(σ)
89	36a″	8.571	CO(πa^p) − Por(π)
	'		
	'		
	'		
91	37a″	8.903	Por(π)
92	38a″	9.253	Por(π)
	'		
	'		
	'		
94	55a′	10.341	Por(π)
	'		
	'		
	'		
101	58a′	12.358	CO(σ) − Fe d_{z^2} − Fe $d_{x^2-y^2}$ − Por(σ)
	'		
	'		
	'		
106	61a′	12.905	CO(σ) + Fe d_{z^2} − Fe $d_{x^2-y^2}$ − Por(σ)
107	62a′	13.255	Fe $d_{x^2-y^2}$ − Por(σ)

[a] See the footnote of Table 3.

the next-HOMO (47a′: 77) and the third-HOMO (30a″: 76) is very small, about 0.18 eV. This is due to the negative charge on the imidazole N3 position. The next-HOMO is a mixture of the Por (π) and Im (σ) orbitals, and the third HOMO is the imidazole π orbital. The imidazole orbitals are very unstabilized in HRPCO for the negative charge on N3. The natures of the LUMO and next-LUMO are similar to those of HbCO. These differences indicate that the VUV spectrum of HRPCO may be affected by the axial imidazole ligand effect.

The orbital shapes of the four orbitals of HbCO and HRPCO are shown in Figure 2. These orbitals are basically the same between HbCO and HRPCO, having porphyrin π nature, although imidazole σ nature mixes a little with the next-HOMO

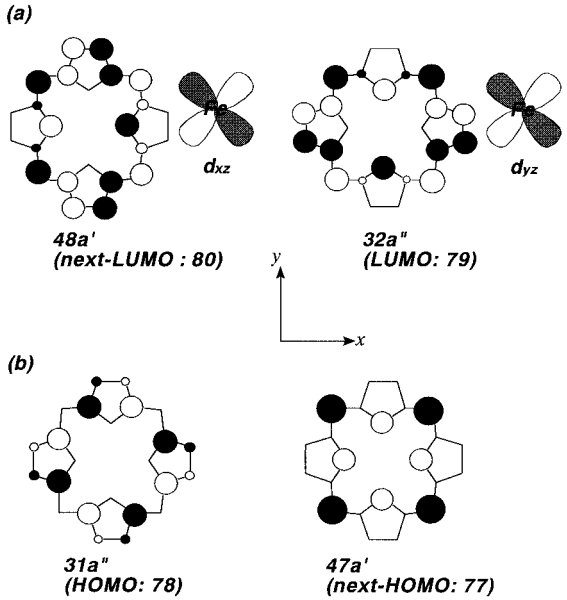

Figure 2. Four orbitals of HbCO and HRPCO: (a) the unoccupied MOs (48a′ and 32a″) and (b) the occupied MOs (31a″ and 47a′).

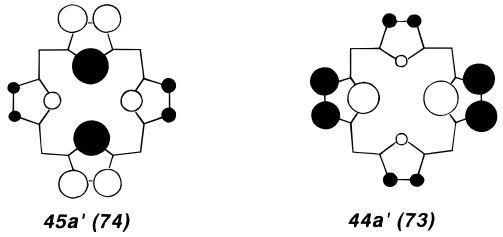

Figure 3. Lower occupied porphyrin π MOs (44a′ and 45a′) which contribute to the main peaks of HbCO.

of HRPCO. In both cases, the components of Fe d_{xz} and d_{yz} orbitals in the two LUMOs are small and the HOMO is an a_{1u}-like orbital and is higher than the a_{2u}-like next-HOMO, in agreement with the results of the NMR[28] and ESR[29] measurements of metalloporphyrin without substituents on the meso position.

In HbCO and HRPCO, the orbitals of the CO ligand do not appear in the MOs in the HOMO−LUMO region. This is in marked contrast to oxyheme. In oxyheme, the oxygen(p)−Fe-(d)π antibonding orbital represents the LUMO and the O_2 π orbital mixes with the HOMO.[22] The bond strength between Fe and the distal ligand, O_2, is small compared to HbCO. Oxyheme also differs from HbCO in the coupling with the imidazole π orbitals.

It is clear from our SAC-CI studies on porphyrins[15,19−22] that the porphyrin π orbitals contribute to the main peaks of the VUV spectra. In Figures 3 and 4 we illustrate some lower occupied MOs of HbCO and HRPCO, respectively, which become important for understanding the electronic spectra of these molecules in the next section. In HbCO, the porphyrin π MOs above 71 do not mix with the imidazole orbitals. On the other hand, in HRPCO, the porphyrin π MOs 70, 72, 74, and 77 (next-HOMO) mix with the imidazolate orbitals and their orbital energies are much raised up. This suggests that the B band energy of HRPCO should be smaller than that of HbCO, as verified in the following section.

Next we analyze the Mulliken population and the bond order of the ground state at the SAC level. The results are shown in Table 5. In HRPCO, a ∼0.18 negative charge is distributed on the Fe, porphyrin ring, and O atom of CO from the proximal imidazolate ligand as compared with HbCO. The transferred charges on the Fe, porphyrin ring, and O atom are about 0.08, 0.06, and 0.03, respectively. In addition, in HRPCO, the Fe−CO and Fe−imidazole bond order increases, the C−O bond order decreases, and the negative charge on the terminal oxygen atom increases in comparison with HbCO, indicating that the anionic proximal ligand accelerates the polarization of the distal CO ligand. Thus, in HRPCO, the C−O bond dissociates a little easier and the Fe−CO bond is a little stronger.

Experimentally, it is known as the so-called "push effect"[30] when the anionic proximal ligand promotes the O−O bond heterolysis of the distal peroxide ligand. For the hetelolytic

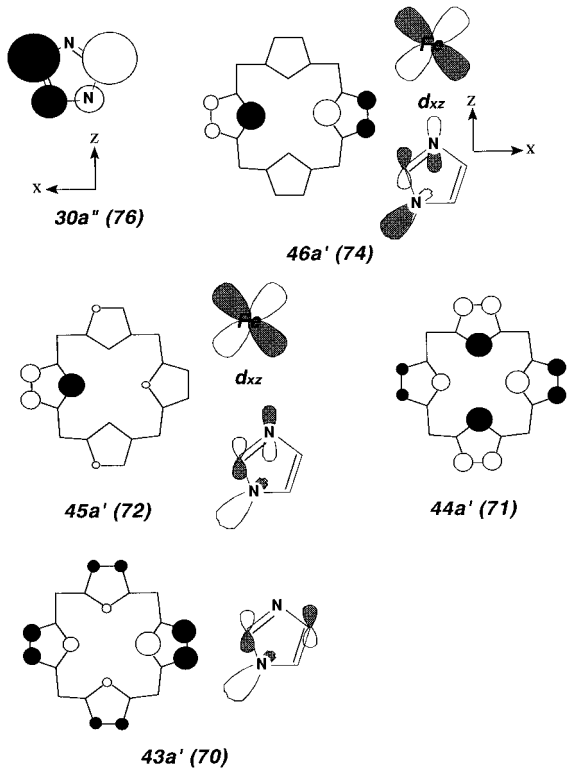

Figure 4. Lower occupied MOs which contribute to the main peaks of HRPCO: the imidazolate π MO (30a″), the porphyrin p MO (44a′), and the porphyrin π + imidazolate σ MOs (43a′, 45a′, and 46a′).

TABLE 5: Mulliken Populations and Bond Orders in the Ground State of HbCO and HRPCO Calculated at the SAC Level

	HbCO	HRPCO
Mulliken Population Analysis		
Fe (net charge)	+1.87	+1.79
d_x	0.22	0.21
d_y	0.22	0.22
d_z	0.23	0.26
d_{xy}	1.98	1.98
d_{xz}	1.92	1.91
d_{yz}	1.93	1.91
C1[a] (net charge)	+0.23	+0.23
p_x	0.59	0.58
p_y	0.56	0.55
p_z	0.98	0.97
O1[a] (net charge)	−0.22	−0.25
p_x	1.51	1.52
p_y	1.51	1.52
p_z	1.37	1.37
Por[b] (net charge)	−1.71	−1.78
Imc (net charge)	−0.17	−0.99
total charge	0.00	−1.00
Mulliken Bond Order Analysis		
Fe−CO	−0.25	−0.23
C−O	0.70	0.69
Fe−Im[c]	−0.05	0.09

[a] The numberings of atoms are given in Figure 1. [b] Porphyrin ring. [c] Imidazole.

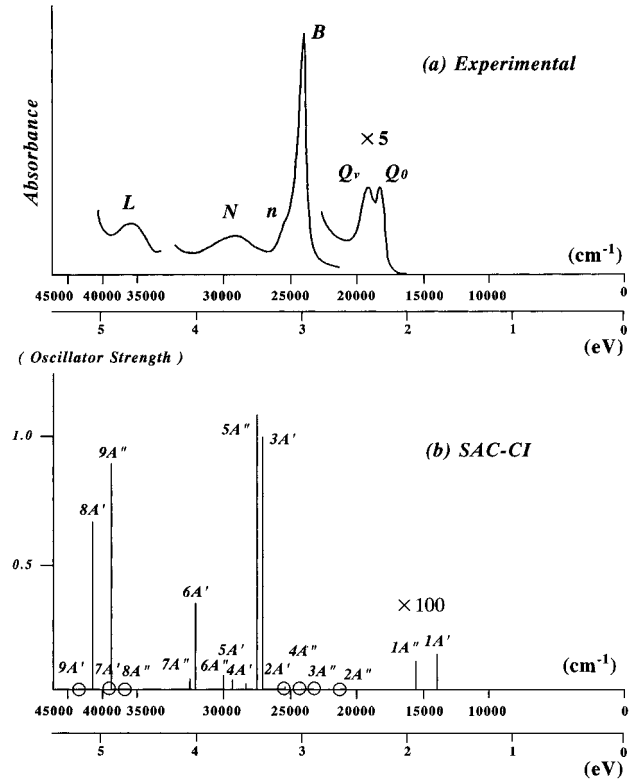

Figure 5. Electronic absorption spectrum of HbCO. (a) Experimental spectrum of horse hemoglobin CO.[31] (b) SAC-CI theoretical spectrum.[15] Open circles indicate singlet states with small oscillator strengths.

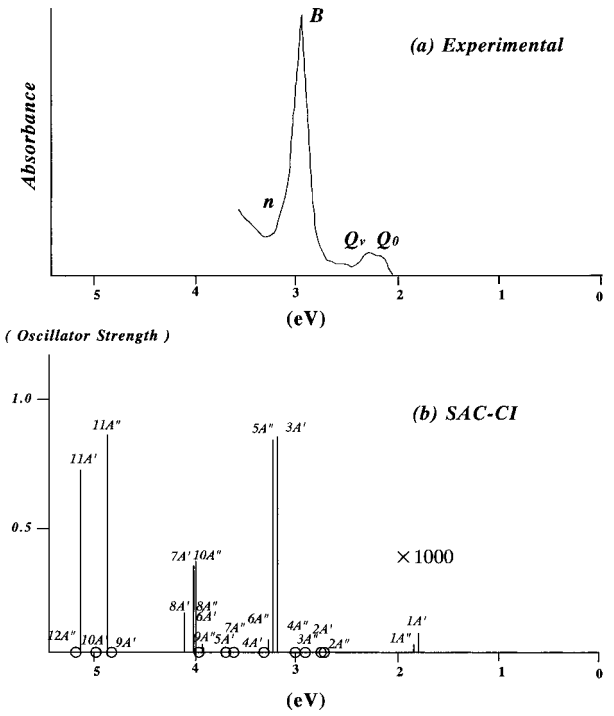

Figure 6. Electronic absorption spectrum of HRPCO: (a) experimental spectrum of horseradish peroxidase CO;[32] (b) SAC-CI theoretical spectrum. Open circles indicate singlet states with small oscillator strengths.

dissociation of the O−O bond, it must be polarized and have a smaller bond order, so that our result is reasonable. Furthermore, it is interesting that the electron charge is almost equally distributed on the Fe atom and on the porphyrin ring. This suggests that compound I of the peroxidases does not easy form Fe(V) oxo porphyrin but the Fe(IV) oxo porphyrin π cation radical after the O−O bond heterolysis. This also agrees with many experimental results.[2, 30e]

IV. Excited States

We calculated the excited states of HbCO and HRPCO in a wide energy range from visible to UV up to 7.8 and 7.1 eV, respectively, although the experimental spectrum covers only up to 4.9 eV for HbCO[31] and only Q and B bands up to 3.6 eV for HRPCO.[32]

Figures 5 and 6 show the experimental electronic absorption spectra of HbCO and HRPCO, respectively, compared with the excitation spectra calculated by the SAC-CI method in the VUV energy region, and Tables 6−9 give more detailed information on the excited states.

The Q_0 and Q_v bands of both HbCO and HRPCO are assigned to the 1A′ and 1A″ states with the polarizations x and y, respectively: the energies and the natures of the excited states are similar between these compounds, implying that the anionic proximal ligand effect is small on the Q bands. A closer examination shows that the Q bands of HRPCO appear at lower energy than those of HbCO, and this is reproduced by the SAC-CI results. These Q bands have very small oscillator strengths

TABLE 6: Excited States of HbCO Lower Than 5.2 eV Calculated by the SAC/SAC-CI Method

SAC-CI						exptl	
state	main configuration ($\|C\|$ > 0.25)	nature[a]	excitation energy (eV)	polarization	oscillator strength	excitation energy (eV)	
1A′	−0.70(77−80)+0.65(78−79)	$\pi-\pi^*$	1.84	x	1.39×10^{-3}	2.18	Q_0
1A″	0.70(77−79)+0.65(78−80)	$\pi-\pi^*$	1.94	y	1.10×10^{-3}	2.30	Q_v
2A″	−0.86(75−79)−0.27(63−79)	$\pi-\pi^*$	2.72	y	1.44×10^{-3}		
3A″	0.55(76−80)+0.47(68−102)+0.42(68−108)+0.23(68−115)	d,π,σ−d*,π^*,σ^*	2.96	y	3.7×10^{-4}		
4A″	−0.68(76−80)+0.40(68−102)+0.36(68−108)	d,π,σ−d*,π^*,σ^*	3.00	y	3×10^{-5}		
2A′	0.64(75−80)−0.58(76−79)	$\pi-\pi^*$	3.15	x	7.42×10^{-3}		
3A′	0.65(78−79)+0.51(77−80)−0.34(74−80)+0.26(73−80)	$\pi-\pi^*$	3.36	x	1.04	2.96	B
5A″	0.66(78−80)−0.53(77−79)−0.39(73−79)	$\pi-\pi^*$	3.41	y	1.13	3.16	n
4A′	0.64(76−79)+0.59(75−80)	$\pi-\pi^*$	3.52	x	1.79×10^{-2}		
5A′	−0.46(63−101)+0.28(63−113)−0.27(75−101)−0.25(63−112)	d,σ−d*,σ^*,CO*	3.63	x	3.59×10^{-2}		
6A″	0.39(62−101)−0.32(69−101)+0.29(76−101)−0.27(64−101)	d,σ−d*,σ^*,CO*	3.72	y	5.44×10^{-2}		
6A′	−0.85(74−80)−0.35(77−80)	$\pi-\pi^*$	3.98	x	0.350	3.60	N
7A″	−0.86(74−79)−0.35(73−79)	$\pi-\pi^*$	4.06	y	3.97×10^{-2}		
8A″	−0.72(68−101)+0.34(68−113)−0.29(68−105)	d,σ−d*,σ^*,CO*	4.65	y	4.3×10^{-4}		
9A″	−0.77(73−79)+0.39(74−79)+0.33(77−79)	$\pi-\pi^*$	4.71	y	0.928	4.53	L
7A′	−0.93(78−81)	$\pi-\pi^*$	5.01	x	5.49×10^{-3}		
8A′	0.91(73−80)	$\pi-\pi^*$	5.12	x	0.655		M

[a] "σ" and "π" denote the porphyrin σ and π MOs, respectively. "d" denotes the Fe d orbital, and "CO*" the CO π and σ antibonding orbital.

TABLE 7: Excited States of HbCO Higher Than 5.2 eV Calculated by the SAC/SAC-CI Method

state	main configuration ($\|C\| > 0.25$)	nature[a]	excitation energy (eV)	polarization	oscillator strength
10A″	0.34(62−101)+0.30(62−108)+0.29(76−102)−0.28(69−102)	d,σ−d*,CO*	5.31	*y*	4×10^{-5}
11A″	0.59(63−79)−0.37(77−81)−0.34(65−79)−0.27(75−79)	d,σ,π−π*	5.54	*y*	6.6×10^{-4}
9A′	0.41(63−102)+0.36(63−108)−0.29(63−101)+0.25(75−102)	d,σ,π−d*,CO*	5.55	*x*,*y*	6.3×10^{-4}
12A″	0.47(62−80)−0.45(69−80)−0.40(63−79)−0.28(64−80)−0.26(76−80)	d,σ−π*	5.63	*y*	2×10^{-5}
13A″	0.81(77−81)	π−π*	5.88	*y*	1.38×10^{-3}
10A′	0.47(62−79)−0.45(69−79)−0.35(76−79)−0.30(63−80)−0.27(64−79)	d,σ−π*	5.91	*z*	2.0×10^{-4}
11A′	−0.56(63−80)−0.39(71−80)+0.33(75−80)+0.28(70−79)	d,π−π*	6.00	*x*,*z*	4.1×10^{-4}
12A′	0.61(71−80)−0.50(70−79)−0.29(63−80)	π−π*	6.11	*x*	8×10^{-5}
14A″	−0.74(71−79)−0.55(70−80)	π−π*	6.14	*y*	0.0
15A″	−0.88(75−81)	d,π−π*	6.49	*y*	0.105
13A′	0.91(76−81)	d,π−π*	6.63	*x*	9.52×10^{-2}
14A′	−0.69(70−79)−0.61(71−80)	π−π*	6.68	*x*	4.1×10^{-4}
16A″	0.72(70−80)−0.56(71−79)	π−π*	6.93	*y*	1×10^{-5}
15A′	−0.76(77−85)−0.54(77−83)	π−d*,CO*	7.33	*x*,*z*	2.83×10^{-2}
17A″	0.77(68−88)−0.52(68−85)	d−CO*	7.34	*y*	4.7×10^{-4}
18A″	0.89(78−83)+0.39(78−85)	π−d*,CO*	7.36	*y*	1.86×10^{-2}
19A″	−0.78(78−86)+0.30(73−81)−0.30(78−85)+0.25(78−83)	π−d*,π*,CO*	7.46	*y*	6.2×10^{-4}
20A″	0.72(70−80)−0.56(71−79)	π−π*	7.47	*y*	3.55×10^{-2}
16A′	0.86(77−86)−0.34(77−83)	π−d*,CO*	7.49	*z*	3.31×10^{-3}
17A′	0.87(78−84)−0.31(78−91)+0.27(78−82)	π−d*,σ*,CO*,Im(π*)[b]	7.61	*x*	4.71×10^{-2}
18A′	−0.79(64−79)+0.37(69−79)	d,σ−π*	7.74	*z*	1.98×10^{-3}

[a] See the footnote of Table 6. [b] "Im(π*)" denotes the imidazole π antibonding orbital.

TABLE 8: Excited States of HRPCO Lower Than 5.2 eV Calculated by the SAC/SAC-CI Method

	SAC-CI					exptl	
state	main configuration ($\|C\| > 0.25$)	nature[a]	excitation energy (eV)	polarization	oscillator strength	excitation energy (eV)	
1A′	0.73(77−80)−0.60(78−79)	π−π*	1.79	*x*	7×10^{-5}	2.17	Q_0
1A″	−0.73(77−79)−0.65(78−80)	π−π*	1.85	*y*	3×10^{-5}	2.29	Q_v
2A″	0.63(74−79)+0.43(72−79)+0.35(73−80)+0.26(64−79)	d,σ,π,Im(σ,π)−π*	2.84	*y*	8.9×10^{-4}		
2A′	−0.74(73−79)+0.30(65−79)−0.30(74−80)−0.25(72−80)	d,σ,π,Im(σ,π)−π*	2.90	*x*	3.9×10^{-4}		
3A″	0.57(73−80)+0.55(75−80)−0.32(74−79)−0.27(65−80)	d,σ,π,Im(σ,π)−π*	2.93	*y*	3.35×10^{-3}		
4A″	−0.65(66−107)+0.50(66−112)+0.39(66−102)	d−d*,σ*	3.01	*y*	6×10^{-5}		
3A′	0.69(78−79)+0.46(77−80)−0.33(72−80)	d,π,Im(σ)−π*	3.19	*x*	0.847	2.93	B
5A″	0.66(78−80)−0.46(77−79)+0.32(72−79)	d,π,Im(σ)−π*	3.22	*y*	0.836	3.16	n
6A″	0.70(75−80)−0.59(73−80)	d,σ,π,Im(π)−p*	3.26	*y*	5.11×10^{-2}		
4A′	0.64(74−80)+0.42(72−80)−0.39(73−79)+0.30(64−80)	d,σ,π,Im(σ,π)−π*	3.38	*x*	1.73×10^{-3}		
7A′	−0.38(65−106)−0.28(61−106)+0.27(73−106)−0.26(65−116)	d,σ,π,Im(π)−d*,σ*,CO*	3.69	*y*	5.47×10^{-3}		
5A′	0.39(71−80)+0.39(64−106)+0.28(64−107)+0.27(64−101)	d,σ,π,Im(π)−d*,CO*	3.86	*x*,*z*	7.83×10^{-3}		
6A′	−0.82(71−80)	π−π*	3.92	*x*	2.77×10^{-2}		
8A″	−0.80(76−80)−0.33(72−79)−0.30(74−79)	d,π,Im(σ,π)−π*	3.92	*y*	1.82×10^{-2}		
9A″	0.78(71−79)+0.42(76−80)	π,Im(π)−π*	3.95	*y*	4.68×10^{-3}		
10A″	−0.54(72−79)+0.41(71−79)+0.39(74−79)−0.36(76−80) −0.27(77−79)	d,π,Im(σ,π)−π*	4.01	*y*	0.361		N
7A′	−0.58(72−80)+0.49(74−80)−0.39(76−79)−0.27(77−80)	d,π,Im(σ,π)−π*	4.02	*x*	0.344		N
8A′	−0.89(76−79)	Im(π)−π*	4.12	*x*	0.152		N
9A′	−0.76(78−81)−0.49(75−79)	σ,π,Im(σ)−π*	4.82	*x*	7.2×10^{-4}		
11A″	0.82(70−79)−0.29(77−79)−0.26(72−79)	d,π,Im(σ)−π*	4.88	*y*	0.860		L
10A′	−0.69(75−70)+0.56(78−81)+0.25(65−79)	d,σ,π,Im(σ)−π*	4.97	*x*,*z*	1.78×10^{-3}		
11A′	0.87(70−80)	π,Im(σ)−π*	5.11	*x*	0.711		M
12A″	−0.64(66−106)−0.42(66−101)+0.41(66−116)	d−d*,σ*,CO*	5.17	*y*	7×10^{-5}		

[a] See the footnote of Table 7. "Im" denotes the imidazolate orbital of the proximal ligand.

($\sim 10^{-3}$ for HbCO and $\sim 10^{-5}$ for HRPCO). In both HbCO and HRPCO, the Q band is formed by a superposition of two configurations. For example, the 1A″ state representing the Q_v band of the HRPCO is described by a superposition of the two configurations, 77 MO → 79 MO and 78 MO → 80 MO, as shown in Table 8, and the absolute values of the coefficients of the two main configurations are approximately equal (e.g., 0.73 and 0.65), reflecting the validity of the four-orbital model. The transition dipole moment is expressed by a sign-reversed superposition of these two configurations, and therefore when the weights of these configurations are equal, the moment is canceled out. Actually, the structures of HbCO and HRPCO in protein should be strained owing to the side chain of the porphyrin ring and the interaction with amino acids near the heme, so that the weights of the two configurations should be more different than those calculated here. We think this is why the Q bands of the SAC-CI calculations are weaker than those of the experiment.

The B (Soret) band and the shoulder band at the higher energy side of HbCO and HRPCO are observed at around 3 eV of the experimental spectra, and they are assigned to the 3A′ and 5A″ states with the polarizations *x* and *y*, respectively, calculated at 3.36 and 3.41 eV for HbCO and 3.19 and 3.22 eV for HRPCO. These two excitations have large oscillator strengths, and the shoulder band is named here as the "n band" (see Figures 5 and 6). Theoretically the n band corresponds to the N band of FBP,[19] which also appears similarly as a shoulder of the B band. This point will be discussed in more detail in section V. In HbCO, the excitations from other lower MOs, 73 and 74 to 79 (LUMO) and 80 (next-LUMO) mix with the excitations within

TABLE 9: Excited States of HRPCO Higher Than 5.2 eV Calculated by the SAC/SAC-CI Method

state	main configuration ($\|C\| > 0.25$)	nature[a]	excitation energy (eV)	polarization	oscillator strength
13A″	−0.38(65−107)+0.31(73−107)+0.29(65−112)−0.27(61−107)	d,σ,π,Im(π)−d*,σ*	5.35	*y*	2.5×10^{-4}
12A′	0.38(64−107)+0.35(66−79)−0.29(64−112)−0.28(64−106)−0.26(64−102)	d,σ,Im(π)−d*,σ*,π*,CO*	5.51	*z*	5×10^{-5}
14A″	−0.62(64−79)−0.53(77−81)	d,σ,π,Im(π)−π*	5.55	*y*	2×10^{-5}
15A″	0.74(77−81)−0.45(64−79)	d,σ,π,Im(π)−π*	5.75	*y*	5.3×10^{-4}
13A′	0.69(64−80)+0.31(66−79)−0.26(74−80)−0.25(72−80)	d,σ,π,Im(π)−π*	5.88	*x*	2.7×10^{-4}
14A′	0.73(66−79)−0.37(64−80)	d,σ,Im(π)−π*	5.90	*x*,*y*	5.9×10^{-4}
15A′	−0.86(73−81)	d,π−π*	6.10	*x*,*z*	7.33×10^{-2}
16A′	0.66(68−79)−0.65(69−80)	π−π*	6.10	*x*,*z*	7.2×10^{-4}
16A′	0.82(65−80)+0.26(73−80)	d,σ,π,Im(π)−π*	6.14	*y*	2×10^{-5}
17A′	0.51(65−79)+0.41(75−79)+0.39(61−79)+0.36(66−79)+0.31(73−79)	d,σ,π,Im(π)−π*	6.17	*x*	2.97×10^{-3}
17A″	−0.88(66−80)	d−π*	6.57	*y*	4.59×10^{-3}
18A″	0.78(74−81)+0.38(72−81)	d,σ,p,Im(π)−π*	6.59	*y*	8.20×10^{-2}
19A′	0.77(77−84)−0.49(67−79)	π,Im(σ)−d*,σ*,π*,CO*	6.80	*y*	1.45×10^{-2}
20A″	0.78(67−79)+0.47(77−84)	π,Im(σ)−d*,σ*,π*,CO*	6.86	*y*	2.63×10^{-2}
18A′	−0.91(67−80)	Im(σ)−π*	6.86	*x*,*z*	2.7×10^{-4}
19A′	0.82(77−83)+0.37(77−82)	π−d*,σ*,CO*	7.10	*x*,*z*	1.37×10^{-2}

[a] See the footnote of Table 8.

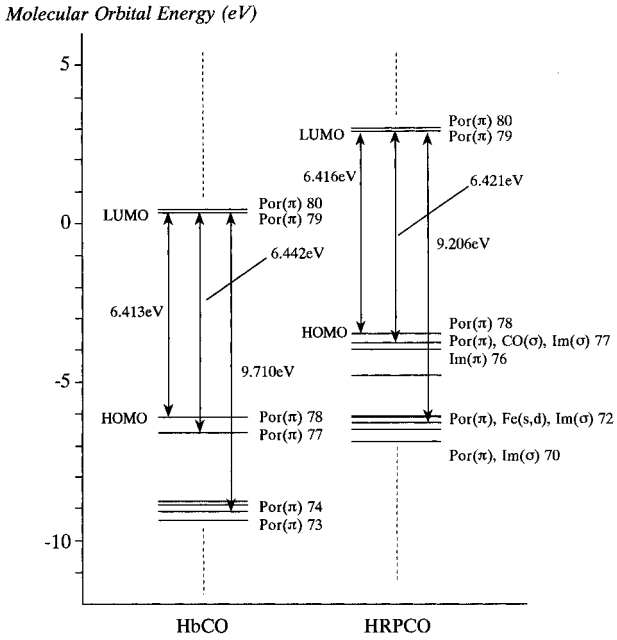

Figure 7. Hartree−Fock MO energies contributing to the main peaks of HbCO and HRPCO.

the four orbitals, and in HRPCO the excitations from MO 72 mix into the B and n bands. This mixing of the lower orbitals in the B and n bands is common to all the porphyrins studied so far[15,19−22] and leads to a breakdown of the four-orbital model, giving a separation of the two nearly degenerate states. In the previous preliminary communication on HbCO,[15] the n band was also called the B band, which should be corrected as above.

In MO 72 of HRPCO, the imidazolate σ nature mixes largely into the porphyrin π nature, so that the MO energy level is raised up. Figure 7 shows the HF energy diagrams of HbCO and HRPCO in the vicinity of the four orbitals. The energy difference between LUMO and the lower mixing MO 72 in HRPCO (9.206 eV) is smaller than the corresponding difference in HbCO (9.710 eV), while the energy difference within the four orbitals is almost the same between these compounds. This is why the B band energies are lower in HRPCO than in HbCO. The experimental difference, 0.03 eV, is smaller than the difference in the SAC-CI results, about 0.18 eV. Actually in the experimental condition the dissociation of the H7 proton of the proximal imidazole ligand of HRPCO should be incomplete, since the H7 proton is actually hydrogen bonded with the proximal asparatic acid residue.[6] Therefore, the extent of destabilization of MO 72 is smaller, so that the lowering of the B band should be smaller. On the other hand, in cytochrome P450s, the proximal ligand is thiolate derived from the cysteine residue,[6] and the B band of the P450CO complex appears at 2.78 eV. The experimental B band energy difference between HbCO and P450CO is 0.18 eV, which is the same as the present theoretical difference between HbCO and HRPCO.

The nature of the N band is different between HbCO and HRPCO, as seen from Tables 6 and 8. In HbCO, the N band consists of only one state, 6A′, polarized in the *x* direction, and the orbitals involved are the same as those of the B band. In HRPCO, on the other hand, three large-intensity states, 10A″, 7A′, and 8A′ polarized in *y*, *x*, and *x* directions, respectively, appear in this energy region, and the orbitals involved are much different from those of the B band: MOs 71, 74, and 76 not involved in the B band participate in HRPCO. In particular, the MO 76 is the imidazolate π^{p} orbital, not a porphyrin π orbital. Therefore, the N band of HRPCO has the nature of a CT (charge transfer) band, an electron being transferred from the imidazolate π space to the porphyrin π space. Thus, the three different components of the N band of HRPCO are characterized by the anionic nature of the imidazolate ligand. The intensity of the N band of HRPCO should be larger than that of HbCO. We think that this N band would be the lower band of the "split Soret" band in P450CO.[33]

The L and M bands of HbCO are assigned to the 9A″ and 8A′ states, respectively, and those of HRPCO to 11A″ and 11A′, respectively. The L band should have the polarization *y* and the M band the polarization *x*. The main excitations of the L and M bands of HbCO are 73 → 79 and 73 → 80, respectively. MO 73 of HbCO and MO 70 of HRPCO are very similar, as seen from Figures 3 and 4, so that the L and M bands of HbCO and HRPCO are quite similar: they are essentially the excitations within the porphyrin π orbitals, although a small mixing of the imidazolate orbital is seen for HRPCO.

The excited states of HbCO and HRPCO lying lower than 5.2 eV summarized above represent the most important part of the excitation spectra. The strong peaks Q, B, n, N, L, etc., all correspond to the excitations to the LUMO and next-LUMO, and the important occupied orbitals are the four orbitals plus some other MOs shown in Figures 2, 3, and 4. Except for the N band of HRPCO, the natures of these excitations are essentially within porphyrin, from por(π) to por(π*). However, we show later that the namings N, L, etc., of the peaks among the spectra of porphyrins by experiment are rather arbitrary. Namely, the name does not reflect the nature of the excited

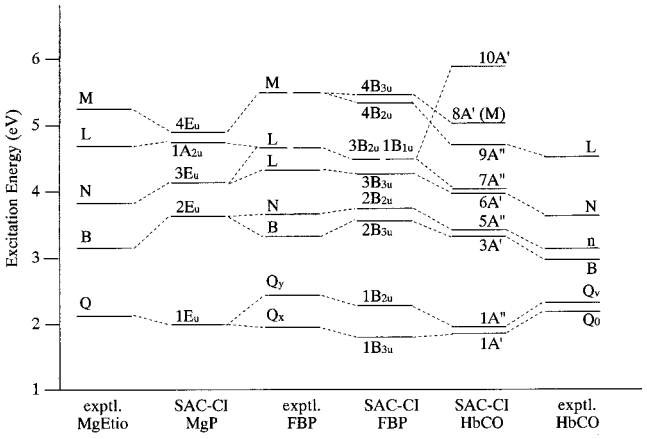

Figure 8. Energy levels of the excited states of FBP, MgP, and HbCO calculated by the SAC-CI method compared with the experimental energy levels observed for FBP, MgEtio (Mg−etioporphyrin), and hemoglobin CO.

state. Therefore, similar excited states of different porphyrins are sometimes called by different names.

The excited states lying higher than 5.2 eV are summarized in Tables 7 and 9 for HbCO and HRPCO, respectively. These excitations are characterized first by the variety of the excitation natures and second by their low intensities. In this higher energy region, the excitations involve many different MOs and the natures of the transitions are characterized as d−π*, π−d*, d−CO*, and π−CO*, in addition to π−π*, and in HRPCO the occupied imidazolate π and σ MOs are also involved. For this reason, the intensities of the transitions in this energy region are small.

In conclusion, the Q, B, n, L, and M bands of HbCO and HRPCO are explained by the excitations within "six orbitals", Gouterman's four orbitals plus MOs 73 and 74 for HbCO and MOs 70 and 72 for HRPCO: as seen from Figures 3 and 4, the MOs 73(HbCO) and 70(HRPCO) are similar, but the MOs 74(HbCO) and 72(HRPCO) are different. Since MO 72 of HRPCO is relatively unstabilized in comparison with MO 74 of HbCO due to a mixing of the imidazolate orbitals, the B band of HRPCO shifts to lower energy. Although the N band of HbCO is formed by the six-orbitals, that of HRPCO is not formed by the six-orbitals: other occupied MOs, in particular, the imidazolate π^{p} MO, also participate in the N band of HRPCO.

V. Nature of the Excited States Compared with Other Porphyrins

As pointed out in the preceding section, the naming of the peaks in the experimental spectra of porphyrins seems to be rather arbitrary. The excited states having similar electronic structures of different porphyrins are sometimes called by different names. We examine here the natures of the excited states of HbCO in comparison with those of free-base porphine (FBP)[19] and Mg−porphine.[20]

Figure 8 shows the experimental and SAC-CI energy levels of FBP, MgP, and HbCO correlated to each other on the basis of the similarity of the main configurations. For HbCO, the SAC-CI result is compared with the experimental peaks of horse hemoglobin CO,[31] and for MgP the SAC-CI result is compared with the experimental peaks of Mg−etioporphyrin. For FBP, we have the gas-phase spectrum of FBP itself,[19] and the agreement between the experimental and SAC-CI peaks was good, so that we gave a new theoretical assignment of the experimental peaks. Note that MgP has D_{4h} symmetry, and some excited states are 2-fold degenerate.

The Q bands consist of a weak peak observed at 2.18 and 2.30 eV for HbCO. By the SAC-CI calculations, the Q bands are assigned to the 1A′ and 1A″ states calculated at 1.84 and 1.94 eV, respectively. The main configurations of the 1A′ and 1A″ states are formed by the four orbitals, and the weights of the two main configurations, 47a′ → 48a′ and 31a″ → 32a″ and 47a′ → 32a″ and 31a″ → 48a′, respectively, are almost the same, as seen from Table 6. The same was true for the $1B_{3u}$ and $1B_{2u}$ states of FBP, which correspond to the 1A′ and 1A″ states, respectively, of HbCO. In the MgP, these two states become degenerate, as the $1E_u$ state. Thus, the Q bands of all of these compounds correspond to the excited states similar to each other and formed by the four π-type orbitals in the HOMO−LUMO region.

The next strong peak, the B band, of HbCO is observed at 2.96 eV in the experimental spectrum. The main configuration of the 3A′ state includes not only the excitations within the four orbitals but also the excitations from the lower MOs 44a′ and 45a′. In FBP the mixing of the excitation from the $4b_{1u}$ MO, which is the 45a′ MO in HbCO, was large; the coefficient was 0.43 in the $2B_{3u}$ state, while in HbCO, the coefficient was 0.34 in the 3A′ state. The 5A″ state of HbCO is assigned to the n band proposed here, which is the B band shoulder at the higher energy region. A similar shoulder peak is called the N band in FBP and was assigned to the $2B_{2u}$ state. These states become degenerate with the B band peak in the D_{4h} symmetry of MgP.

On the other hand, the next N band of HbCO is assigned to the 6A′ state. This state corresponds to the lower L band, $3B_{3u}$ state, of FBP because they have an *x* polarization and their major configurations are composed of the excitations from the MOs lower than the four orbitals. The higher L band, $3B_{2u}$ state, of FBP is comparable with the 7A″ state of HbCO: they commonly have a *y* polarization and small oscillator strengths. In addition, another higher L band, $1B_{1u}$ state, of FBP corresponds to the 10A′ state of HbCO, because they have n−π* nature and *z* polarization. The three L band states in FBP become N (degenerate $3E_u$) and L (1^1A_{2u}) bands of MgP.

The L band, 9A″ state, of HbCO is different in nature from the L bands of FBP, but corresponds to the lower M band, $4B_{2u}$ state, of FBP. The M band, 8A′ state, of HbCO is comparable with the higher M band, $4B_{3u}$ state, of FBP. The two almost degenerate M bands of FBP become the M band (degenerate $4E_u$) in MgP. Thus, the excited states having similar electronic structures are called by different names in different porphyrins, and the relations are summarized in Figure 8.

VI. Conclusions

The ground and excited states of HbCO and HRPCO were studied by the SAC/SAC-CI method, and the results are summarized as follows.

(1) The ground states of HbCO and HRPCO are Fe(II) low-spin ($S = 0$) closed shell states. In HRPCO, a ∼0.18 anionic charge is distributed on the Fe atom, porphyrin ring, and O atom of the distal CO ligand from the proximal imidazolate ligand in comparison with HbCO. In addition, the anionic proximal ligand works to increase the Fe−CO and Fe−imidazole bond orders and decrease the distal C−O bond order. These results imply that the anion nature of the proximal ligand can be responsible for the enzymatic activity, although the distal ligand is not a peroxide, which is an enzymatic cycle model.

(2) The calculated results for the excitation energy and the oscillator strength correspond well with the experimental spectra.

(3) In HbCO and HRPCO, the Q_0 and Q_v peaks are assigned to the 1A′ and 1A″ states, respectively. These bands are explained by the excitations within Gouteman's four orbitals.

(4) In both compounds, the B band shoulder at the higher energy side is named the "n band", which is a counterpart of the B band in the limit of the four-orbital model.

(5) In HbCO, the B, n, N, L, and M bands are described by the excitations within the "six orbitals", two lower occupied MOs 73 and 74 being added to the four orbitals. All six orbitals are porphine π MOs.

(6) In HRPCO, the B, n, L, and M bands are also described by the excitations within the "six orbitals", two lower occupied MOs 70 and 72 being added to the four orbitals. These six orbitals are also porphine π MOs, although in MO 72 the mixing of the imidazolate orbitals is considerable.

(7) In HbCO, the B and n bands are assigned to the 3A′ and 5A″ states, respectively. In both bands, the excitations within the four orbitals are larger than those from the two lower orbitals. In the N and L bands, the weights of the excitations within the four orbitals are smaller than those of the other configurations in the six-orbital model. In the M bands, the weights of the four orbitals are very small.

(8) In HRPCO, the B and n bands are also assigned to the 3A′ and 5A″ states, respectively. In both bands, the excitations within the four orbitals are larger than those from the other two. However, since the MO 72 is raised up considerably by the anionic nature of imidazolate, the B and n band energies of HRPCO are lower than those of HbCO. In the N and L band, the weights of the excitations within the four orbitals are smaller than those of the other MOs, and in the M band the four-orbital contributions are very small.

(9) The nature of the N band of HRPCO is considerably different from that of HbCO. The N band of HbCO is *x*-polarized porphine π-π* excitations, while that of HRPCO consists of three peaks polarized in *y*, *x*, and *x* directions in increasing energy order, and the charge transfer nature is especially prominent in the highest *x*-polarized peak. The intensity of the N band of HRPCO should be larger than that of HbCO.

(10) In the energy region higher than 5.2 eV, there are a number of excited states having a variety of excitation natures, $\pi-\pi^*$, d$-\pi^*$, $\pi-$d*, d$-$CO*, $\pi-$CO*, etc. However, no strong peaks are predicted in this region.

(11) The namings of the peaks in the experimental spectra of porphyrins are rather arbitrary. The excited states having similar electronic structures are sometimes called by different names in different porphyrins. The correspondence diagram was given in Figure 8 for FBP, HbCO, and MgP.

Acknowledgment. We thank Dr. M. Hada and Mr. J. Hasegawa for discussions and valuable advice on the computations. This study has been partially supported by a Grant-in-Aid for Scientific Research from the Japanese Ministry of Education, Science, and Culture and by the New Energy and Industrial Technology Development Organization (NEDO).

References and Notes

(1) Saunders, B. C.; Holmes-Siedle, A. G.; Stark, B. P. In *Peroxidases*; Butterworth: Washington, DC.

(2) (a) Dolphin, D.; Forman, A; Borg, D. C.; Fajer, J.; Felton, R. H. *Proc. Natl. Acad. Sci. U.S.A.* **1971**, *68*, 614. (b) La Mar, G.; de Ropp, J. S.; Smith, K. M.; Langry, K. C. *J. Biol. Chem.* **1981**, *256*, 237. (c) Roberts, J. E.; Hoffmann, B. M.; Rutter, R.; Hager, L. P. *J. Biol. Chem.* **1981**, *256*, 2118. (d) Hanson, L. K.; Chang, C. K.; Davis, M. S.; Fajer, J. *J. Am. Chem. Soc.* **1981**, *103*, 663. (e) Dawson, J. H.; Holm, R. H.; Trudell, J. R.; Barth, G.; Linder, R. E.; Bunnenberg, E.; Djerassi, C.; Tang, S. C. *J. Am. Chem. Soc.* **1976**, *98*, 3707.

(3) (a) Hewson, W. D.; Hager, L. P. *J. Biol. Chem.* **1979**, *254*, 3182. (b) Hayashi, Y.; Yamazaki, I.; *J. Biol. Chem.* **1979**, *254*, 9101.

(4) Groves, J. T.; Haushalter, R. C.; Nakamura, M.; Nemo, T. E.; Evans, B. J. *J. Am. Chem. Soc.* **1981**, *103*, 2884.

(5) Finzel, B. C.; Poulos, T. L.; Kraut, J. *J. Biol. Chem.* **1984**, *259*, 13027.

(6) Poulos, T. L.; Finzel, B. C.; Howard, A. J. *Biochemistry* **1986**, *25*, 5314.

(7) Springer, B. A.; Silger, S. G.; Olson, J. S.; Phillips, G. N., Jr. *Chem. Rev.* **1994**, *94*, 699.

(8) Phillips, S. E. V.; Schoenborn, B. P. *Nature* **1981**, *292*, 81.

(9) (a) Derewenda, Z.; Dodson, G.; Emsley, P.; Harris, D.; Nagai, K.; Perutz, M.; Reynaud, J.-P. *J. Mol. Biol.* **1990**, *211*, 515. (b) Baldwin, J. M. *J. Mol. Biol.* **1980**, *136*, 103.

(10) (a) Tsubaki, M.; Srivastava, R. B.; Yu, N.-T. *Biochemistry* **1982**, *21*, 1132. (b) Li, X. Y.; Spiro, T. G. *J. Am. Chem. Soc.* **1988**, *110*, 6024. (c) Hirota, S.; Ogura, T.; Shinzawa, K.; Itoh, K.; Yoshikawa, S.; Nagai, M.; Kitagawa, T. *J. Phys. Chem.* **1994**, *98*, 6652.

(11) Case, D. A.; Huynh, B. H.; Karplus, M. *J. Am. Chem. Soc.* **1979**, *16*, 4433.

(12) Loew, G. H.; Rohmer, M.-M. *J. Am. Chem. Soc.* **1980**, *102*, 3655.

(13) (a) Jewsbury, P.; Yamamoto, S.; Minato, T.; Saito, M.; Kitagawa, T. *J. Phys. Chem.* **1995**, *99*, 12677. (b) Ghosh, A.; Bocian, D. F. *J. Phys. Chem.* **1996**, *100*, 6363.

(14) Obara, S.; Kashiwagi, H. *J. Chem. Phys.* **1982**, *79*, 3155.

(15) Nakatsuji, H.; Tokita, Y.; Hasegawa, J.; Hada, M. *Chem. Phys. Lett.* **1996**, *256*, 220.

(16) (a) Nakatsuji, H. In *Computational Chemistry—Reviews of Recent trends, Vol. 2: SAC-CI Method: Theoretical Aspects and Some Recent Topics*; Leszczynski, J., Ed.; World Scientific: Singapore, in press. (b) Nakatsuji, H. *Acta. Chim. Hung.* **1992**, *129*, 719.

(17) Nakatsuji, H.; Hirao, K. *J. Chem. Phys.* **1978**, *68*, 2053.

(18) (a) Nakatsuji, H. *Chem. Phys. Lett.* **1978**, *59*, 362. (b) Nakatsuji, H. *Chem. Phys. Lett.* **1979**, *67*, 329, 334.

(19) Nakatsuji, H.; Hasegawa, J.; Hada, M. *J. Chem. Phys.* **1996**, *104*, 2321.

(20) Hasegawa, J.; Hada, M.; Nonoguchi, M.; Nakatsuji, H. *Chem. Phys. Lett.* **1996**, *250*, 159.

(21) (a) Toyota, K.; Hasegawa, J.; Nakatsuji, H. *Chem. Phys. Lett.* **1996**, *250*, 437. (b) Toyota, K.; Hasegawa, J.; Nakatsuji, H. *J. Phys. Chem.*, in press

(22) Nakatsuji, H.; Hasegawa, J.; Ueda, H.; Hada, M. *Chem. Phys. Lett.* **1996**, *250*, 379.

(23) (a) Nakatsuji, H. Program system for SAC and SAC-CI calculations, Program. Library No. 146 (Y4/SAC), Data Processing Center of Kyoto University, 1985; Program Library SAC85, No. 1396, Computer Center of the Institute for Molecular Science, Okazaki, 1981. (b) Nakatsuji, H.; Hada, M.; Hasegawa, J.; Nakai, H. The modified version of SAC85, to be published.

(24) Huzinaga, S.; Andzelm, J.; Klobukowski, M.; Radzio-Andzelm, E.; Sakai, E.; Takewaki, H. *Gaussian Basis Set for Molecular Calculation*; Elsevier: New York, 1984.

(25) Huzinaga, S. *J. Chem. Phys.* **1965**, *42*, 1293.

(26) Nakatsuji, H. *Chem. Phys.* **1983**, *75*, 425.

(27) Gouterman, M. *The Porphyrins*; Dolphin, D., Ed.; Academic: New York, 1977; Vol. III.

(28) (a) Morishima, I.; Takamuki, Y.; Shiro, Y. *J. Am. Chem. Soc.* **1984**, *106*, 7666. (b) Tokita, Y.; Yamaguchi, K.; Watanabe, Y.; Morishima, I. *Inorg. Chem.* **1993**, *32*, 329.

(29) (a) Fajer, J.; Borg, D. C.; Furman, A.; Dolphin, D.; Felton, R. H. *J. Am. Chem. Soc.* **1970**, *92*, 3451. (b) Satoh, M.; Ohba, Y.; Yamaguchi, S.; Iwaizumi, M. *Inorg. Chem.* **1992**, *31*, 298.

(30) (a) Poulos, T. L.; Finzel, B. C.; Gunsalus, I. C.; Wagner, G. C.; Kraut, J. *J. Biol. Chem.* **1985**, *260*, 16122. (b) Thanabal, V.; de Ropp, J. S.; La Mar, G. N. *J. Am. Chem. Soc.* **1988**, *110*, 3027. (c) Murthy, M. R. N.; Reid, T. J., III; Sicignano, A.; Tanaka, N.; Rossmann, M. G. *J. Mol. Biol.* **1981**, *152*, 465. (d) Poulos, T. L.; Howard, A. J. *Biochemistry* **1986**, *25*, 5314. (e) Yamaguchi, K.; Watanabe, Y.; Morishima, I. *J. Am. Chem. Soc.* **1993**, *115*, 4058.

(31) Makinen, M. W.; Eaton, W. A. *Ann. N.Y. Acad. Sci.* **1973**, *206*, 210.

(32) Nozawa, T.; Kobayashi, N.; Hatano, M. *Biochim. Biophys. Acta* **1976**, *427*, 652.

(33) Omura, T.; Sato, R. *J. Biol. Chem.* **1962**, *237*, 1375.